Electronic Supplementary Material (ESI) for Dalton Transactions.

Supplementary Information

SMM features of a large lanthanide family of butterfly $Cr^{III}_2Ln^{III}_2$ pivalate complexes (Ln=Gd, Tb, Dy, Ho, Er, Tm and Yb)

Daiana Cabrosi[a], Juan H. Mecchia Ortiz[a], Luca M. Carrella[b], Eva Rentschler[b] and Pablo Alborés[a]*

[a] Departamento de Química Inorgánica, Analítica y Química Física/ INQUIMAE (CONICET), Facultad de Ciencias Exactas y Naturales Universidad de Buenos Aires, Pabellón 2, Ciudad Universitaria, C1428EHA Buenos Aires, Argentina
Fax: +5411 / 4576-3341
E-mail: albores@qi.fcen.uba.ar

[b] Department Chemie, Johannes Gutenberg Universität Mainz, Duesbergweg 10-12, D-55128 Mainz, Germany.

Table S1. Crystallographic data of complexes **4-8**.

	4	**5**	**6**	**7**	**8**
Empirical Formula	$C_{44}H_{86}Cr_2Tb_2N_2O_{20}$	$C_{44}H_{86}Cr_2Ho_2N_2O_{20}$	$C_{44}H_{86}Cr_2Er_2N_2O_{20}$	$C_{44}H_{86}Cr_2Tm_2N_2O_{20}$	$C_{44}H_{86}Cr_2Yb_2N_2O_{20}$
Formula weight (g/mol)	1385	1397	1401.66	1405	1413.22
T (K)	298(2)	298(2)	298(2)	298(2)	298(2)
Crystal system	Triclinic	Triclinic	Triclinic	Triclinic	Triclinic
Space Group	P-1	P-1	P-1	P-1	P-1
a (Å)	11.1421(5)	11.1437(4)	11.1602(5)	11.1582(4)	11.1858(8)
b (Å)	11.3002(4)	11.2605(5)	11.2588(5)	11.2288(4)	11.2445(6)
c (Å)	12.3000(3)	12.2413(5)	12.2291(5)	12.2148(4)	12.2084(6)
α (°)	105.975(3)	106.323(4)	106.575(4)	106.728(3)	106.881(5)
β (°)	90.898(3)	90.948(3)	91.167(4)	91.108(3)	91.234(5)
γ (°)	94.388(3)	94.054(3)	93.723(4)	93.631(3)	93.317(5)
V (Å^3)	1483.41(9)	1469.43(10)	1468.44(12)	1461.59(9)	1465.74(15)
Z	1	1	1	1	1
D_{calc} (mg/m^3)	1.550	1.579	1.585	1.596	1.601
Absorption coefficient (mm^{-1})	2.778	3.090	3.256	3.434	3.589
F(000)	702	706	708	710	712
λ (Å)	0.71073	0.71073	0.71073	0.71073	0.71073
θ Range data collection (°)	3.67- 26.31	3.84-28.74	3.86-27.71	3.79-28.62	4.01-28.60
Index ranges	-14≤ h ≤13	-14≤ h ≤14	-14≤ h ≤14	-14≤ h ≤13	-14≤ h ≤13
	-14 ≤ k ≤14	-14≤ k ≤14	-14≤ k ≤14	-14≤ k ≤14	-14 ≤ k ≤14
	-15≤ l ≤15	-15≤ l ≤15	-15≤ l ≤15	-15≤ l ≤15	-15≤ l ≤13
Reflections collected/unique	30931/6431	30724/6382	11491/6301	24730/6348	11631
Rint	0.0410	0.0578	0.0424	0.0375	0.0419
Observed reflections [I>2σ(I)]	5773	5647	5405	5798	5700
Completeness (%)	99.74	99.73	99.68	99.72	99.70
Maximum / minimum transmission	1.000/ 0.640	1.000/0.856	1.000/0.934	1.000/0.541	1.000/0.687
Data/restraints/parameters	6431/217/328	6382/205/328	6301/199/328	6348/208/328	6617/205/328
Goodness-of-fit (GOF) on F^2	1.077	1.095	1.050	1.074	1.057
Final R-index [I>2σ(I)]/ all data	0.0392/0.0457	0.0376/0.0452	0.0399/0.503	0.0368/0.0416	0.0413/0.0516
wR index [I>2σ(I)] /all data	0.1055/0.1128	0.0376/0.0452	0.0934/0.1029	0.0975/0.1025	0.0983/0.1077

Largest peak and hole (e A^{-3})	3.002 and -1.701	1.171 and -1.294	1.089 and -1.290	2.814 and -1.792	1.215 and -1.583
Weights, *w*	$1/[\sigma^2(Fo^2)+(0.0569P)^2+5.2438P]$; $P=(Fo^2+2Fc^2)/3$	$1/[\sigma^2(Fo^2)+(0.0431P)^2+2.6984P]$; $P=(Fo^2+2Fc^2)/3$	$1/[\sigma^2(Fo^2)+(0.0381P)^2+2.6038P]$; $P=(Fo^2+2Fc^2)/3$	$1/[\sigma^2(Fo^2)+(0.0518P)^2+5.0765P]$; $P=(Fo^2+2Fc^2)/3$	$1/[\sigma^2(Fo^2)+(0.0455P)^2+1.7781P]$; $P=(Fo^2+2Fc^2)/3$

Table S2. Main bond distances (Å) of complexes **4-8**.

4			**5**			**6**			**7**			**8**		
Tb1	**O2**	2.275(4)	**Ho1**	**O2**	2.249(4)	**Er1**	**O2**	2.232(4)	**Tm1**	**O2**	2.223(4)	**Yb1**	**O2**	2.211(3)
Tb1	**O3**	2.277(3)	**Ho1**	**O3**	2.247(3)	**Er1**	**O3**	2.239(3)	**Tm1**	**O3**	2.222(3)	**Yb1**	**O3**	2.213(4)
Tb1	**O5**	2.379(3)	**Ho1**	**O5**	2.351(3)	**Er1**	**O5**	2.350(3)	**Tm1**	**O5**	2.326(3)	**Yb1**	**O5**	2.333(3)
Tb1	**O7**	2.389(3)	**Ho1**	**O7**	2.362(3)	**Er1**	**O7**	2.336(3)	**Tm1**	**O7**	2.337(3)	**Yb1**	**O7**	2.319(4)
Tb1	**O8**	2.460(4)	**Ho1**	**O8**	2.363(3)	**Er1**	**O8**	2.425(5)	**Tm1**	**O8**	2.341(4)	**Yb1**	**O8**	2.410(5)
Tb1	**O9**	2.396(4)	**Ho1**	**O9**	2.436(4)	**Er1**	**O9**	2.358(5)	**Tm1**	**O9**	2.413(4)	**Yb1**	**O9**	2.335(5)
Tb1	**O10**	2.504(4)	**Ho1**	**O10**	2.481(4)	**Er1**	**O10**	2.472(4)	**Tm1**	**O10**	2.462(4)	**Yb1**	**O10**	2.459(4)
Tb1	**O10'**	2.521(3)	**Ho1**	**O10'**	2.500(3)	**Er1**	**O10'**	2.487(3)	**Tm1**	**O10'**	2.481(3)	**Yb1**	**O10'**	2.474(3)
Cr1	**N1**	2.118(4)	**Cr1**	**N1**	2.109(4)	**Cr1**	**N1**	2.111(5)	**Cr1**	**N1**	2.112(4)	**Cr1**	**N1**	2.112(5)
Cr1	**O2**	1.952(3)	**Cr1**	**O2**	1.947(3)	**Cr1**	**O2**	1.948(3)	**Cr1**	**O2**	1.949(3)	**Cr1**	**O2**	1.955(4)
Cr1	**O3**	1.960(4)	**Cr1**	**O3**	1.957(4)	**Cr1**	**O3**	1.955(4)	**Cr1**	**O3**	1.951(4)	**Cr1**	**O3**	1.945(3)
Cr1	**O4**	1.986(3)	**Cr1**	**O4**	1.981(3)	**Cr1**	**O4**	1.984(4)	**Cr1**	**O4**	1.983(3)	**Cr1**	**O4**	1.984(4)
Cr1	**O6**	1.980(4)	**Cr1**	**O6**	1.982(4)	**Cr1**	**O6**	1.980(3)	**Cr1**	**O6**	1.975(4)	**Cr1**	**O6**	1.985(4)
Cr1	**O10**	1.967(4)	**Cr1**	**O10**	1.968(4)	**Cr1**	**O10**	1.963(4)	**Cr1**	**O10**	1.964(4)	**Cr1**	**O10**	1.961(4)

Table S3. Local Ln(III) *g*-tensor, energies and composition arising from *ab-initio* computation of complexes **4-8**.

{Cr_2Tb_2}				
E / cm^{-1}	g_x	g_y	g_z	Composition
0	0	0	17.42	92% mj = 6
0.4				7% mj = 4
130.3	0	0	13.34	78% mj= 5
131.8				19% mj= 3
247.6	0	0	9.50	53% mj= 4
262.6				31% mj= 2
330.1				
402.4	0	0	12.27	
418.5				
500.1	0	0	16.14	
503.5				
703.0	0	0	17.63	
703.9				

{Cr_2Ho_2}				
E / cm^{-1}	g_x	g_y	g_z	Composition
0	0	0	19.11	90% mj= 8
0.2				
94.6				
119.8	0	0	13.7	
124.7				
151.5	0	0	9.24	
154.8				
197.8	0	0	7.57	
233.4				
252.7	0	0	6.79	
255.4				
270.5	0	0	11.11	
281.2				
332.2	0	0	18.46	
332.3				
390.2	0	0	18.18	
392.1				

{Cr_2Er_2}				
E / cm^{-1}	g_x	g_y	g_z	Composition
0	0.12	0.58	16.30	69% mj=15/2
0				18% mj=11/2
47.8	0.25	0.38	16.23	69% mj=13/2
47.8				15% mj=15/2
				10% mj=11/2
95.2	1.87	2.76	12.11	
95.2				
127.8	1.98	3.63	11.39	
127.8				
183.1	1.39	4.87	10.23	
183.1				
232.1	0.30	3.95	8.72	
232.1				
269.5	9.50	7.05	2.48	
269.5				
380.1	0.26	0.29	17.17	
380.1				

{Cr_2Tm_2}				
E / cm^{-1}	g_x	g_y	g_z	Composition
0	0	0	13.82	97% mj=6
0.7				
279.9	0	0	10.39	68% mj=5 15% mj=4
294.1				
317.1	0	0	8.84	40% mj=4 45% mj=3
362.8				
402.0				
454.7	0	0	11.02	
489.7				
570.2	0	0	11.22	
576.9				
676.2	0	0	13.89	
676.7				

{Cr_2Yb_2}				
E / cm^{-1}	g_x	g_y	g_z	Composition
0	0.65	1.25	7.33	87% mj=7/2 7% mj= 3/2
0				
250.0	1.0	1.02	6.40	57% mj= 5/2 28% mj= 3/2
250.0				
402.5	1.71	2.22	4.50	
402.5				
628.4	0.09	0.16	7.52	
628.4				

Table S4. Angles (degrees) between $g_{Dy,z}$ and $g_{Ln,z}$

	2-Ln angle / degrees
Tb	25
Dy	0
Ho	4
Er	103
Tm	64
Yb	92

Table S5. *Ab-initio* computed low lying doublets energies, *g*-tensors and tunneling splitting of complexes **4-7**.

{Cr_2Tb_2}				
E / cm^{-1}	g_x	g_y	g_z	Δ_{tun}
0.000	0.00	0.00	23.06	<1e-10
0.000				
15.369	0.00	0.00	26.98	1.5e-7
15.369				
15.393	0.00	0.00	26.98	1.0e-7
15.393				
30.106	0.00	0.00	30.87	6.9e-5
30.106				
30.107	0.00	0.00	30.87	5.3e-5
30.107				
30.742	0.00	0.00	30.87	8.4e-5
30.742				
36.774	0.00	0.00	0.00	5.3e-3
36.780				
36.948	0.00	0.00	0.00	2.6e-4
36.948				
36.984	0.00	0.00	0.00	1.0e-2
36.984				
37.174	0.00	0.00	0.00	6.9e-3
37.181				

{Cr_2Ho_2}				
E / cm^{-1}	g_x	g_y	g_z	Δ_{tun}
0.000	0.00	0.00	26.44	2.0e-10
0.000				
10.554	0.00	0.00	30.37	1.3e-7
10.554				
10.570	0.00	0.00	30.37	2.6e-7
10.570				
20.761	0.00	0.00	34.30	1.5e-5
20.761				
20.762	0.00	0.00	34.30	6.0e-6
20.762				
21.095	0.00	0.00	34.30	5.8e-5
21.095				
28.188	0.00	0.00	0.00	4.1e-3
28.192				
28.519	0.00	0.00	0.00	6.7e-4
28.520				
28.586	0.00	0.00	0.00	7.4e-3
28.593				
28.900	0.00	0.00	0.00	7.6e-3
28.907				

{Cr_2Er_2}				
E / cm^{-1}	g_x	g_y	g_z	Δ_{tun}
0.000	0.00	0.00	20.80	2.4e-5
0.000				
6.732	0.00	0.00	24.69	2.3e-3
6.734				
6.760	0.00	0.00	24.72	5.2e-5
6.760				
13.356	0.00	0.00	26.08	1.3e-1
13.490				
13.642	0.00	0.00	0.00	6.1e-2
13.702				
13.752	0.00	0.00	0.00	6.4e-4
13.753				

{Cr_2Tm_2}				
E / cm^{-1}	g_x	g_y	g_z	Δ_{tun}
0.000	0.00	0.00	15.81	3.0e-6
0.000				
4.104	0.00	0.00	19.69	6.0e-4
4.104				
4.127	0.00	0.00	19.69	4.6e-4
4.127				
8.220	0.00	0.00	23.31	3.7e-3
8.224				
8.609	0.00	0.00	0.00	3.3e-4
8.609				
8.610	0.00	0.00	0.00	4.2e-5
8.610				
11.888	0.00	0.00	0.00	6.4e-2
11.952				

Table S6. *Ab-initio* computed main values (J_z assigned to maximum value) dipolar interaction in complexes **4-7**. Ln-Ln interaction corresponds to *s*=1/2 sites and Cr-Ln corresponds to *S*=3/2 and *s*=1/2 sites.

	J_{dip} Ln-Ln (x,y,z) / cm^{-1}	J_{dip} Cr-Ln (x,y,z) / cm^{-1}
4	0, 0, -0.58	0, 0, -0.06 0, -0.01, 0.09
5	0, 0.31, -2.10	0, -0.01, 0.12 0, 0.12, -0.14
6	0, 0, -1.55	0, 0.7, -0.11 0, 0.03, -0.11
7	0, 0, -1.13	0, 0.01, -0.11 0, 0.01, -0.12

Table S7. Best fitting parameters of AC magnetic data, according to Debye model for a single relaxation process of complexes **4-7**.

$\{Cr_2Tb_2\}$				
T / K	χ_S / cm^3mol^{-1}	χ_T / cm^3mol^{-1}	α	τ / s
3.50	1.79E-01	4.57	9.21E-02	6.93E-02
3.70	1.93E-01	4.26	6.54E-02	3.14E-02
3.90	1.97E-01	4.02	6.28E-02	1.55E-02
4.10	1.88E-01	3.83	6.73E-02	7.88E-03
4.30	1.88E-01	3.65	6.21E-02	4.18E-03
4.50	2.08E-01	3.48	4.20E-02	2.30E-03
4.70	2.07E-01	3.37	5.01E-02	1.37E-03
4.90	1.94E-01	3.24	5.58E-02	8.21E-04
5.10	1.78E-01	3.11	5.54E-02	5.04E-04
5.30	2.26E-01	2.99	3.53E-02	3.31E-04
5.50	2.84E-01	2.89	1.95E-02	2.26E-04
5.70	4.13E-01	2.80	4.34E-13	1.66E-04
5.90	4.97E-01	2.72	3.72E-19	1.22E-04
6.10	5.46E-01	2.64	2.33E-12	8.95E-05
Temperature-dependent AC data under 0 Oe applied field.				

{Cr_2Ho_2}				
T / K	χ_S / cm^3mol^{-1}	χ_T / cm^3mol^{-1}	α	τ / s
2.60	2.23E-01	9.48	9.47E-02	1.35E-01
2.70	2.15E-01	9.02	9.34E-02	7.61E-02
2.80	2.07E-01	8.64	9.35E-02	4.40E-02
2.90	1.96E-01	8.31	9.47E-02	2.61E-02
3.00	1.84E-01	8.01	9.53E-02	1.58E-02
3.10	1.70E-01	7.73	9.61E-02	9.76E-03
3.20	1.55E-01	7.49	9.65E-02	6.18E-03
3.30	1.42E-01	7.26	9.53E-02	3.99E-03
3.40	1.26E-01	7.05	9.48E-02	2.63E-03
3.50	1.12E-01	6.85	9.34E-02	1.77E-03
3.70	8.54E-02	6.49	8.95E-02	8.53E-04
3.90	5.19E-02	6.19	8.91E-02	4.40E-04
4.10	6.57E-03	5.92	9.30E-02	2.39E-04
4.30	1.58E-13	5.67	1.03E-01	1.36E-04
Temperature-dependent AC data under 0 Oe applied field.				

{Cr_2Tm_2}				
T / K	χ_S / cm^3mol^{-1}	χ_T / cm^3mol^{-1}	α	τ / s
1.90	6.62E-01	4.48	6.05E-02	3.25E-04
2.00	8.47E-01	4.32	3.55E-02	1.90E-04
2.10	1.13	4.20	1.46E-02	1.32E-04
2.20	1.52	4.09	6.82E-14	1.00E-04
Temperature-dependent AC data under 1400 Oe applied field.				

{Cr_2Er_2}				
T / K	χ_S / cm^3mol^{-1}	χ_T / cm^3mol^{-1}	α	τ / s
1.90	9.04E-01	6.80	1.33E-01	5.60E-04
2.00	1.11	6.43	8.92E-02	3.45E-04
2.10	1.33	6.15	5.56E-02	2.39E-04
2.20	1.63	5.91	2.17E-02	1.75E-04
2.30	1.93	5.69	3.21E-16	1.32E-04
2.40	2.23	5.50	4.90E-13	1.01E-04
Temperature-dependent AC data under 600 Oe applied field.				

{Cr_2Tm_2}				
H / T	χ_S / cm^3mol^{-1}	χ_T / cm^3mol^{-1}	α	τ / s
600	1.79	4.78	2.22E-18	1.13E-04
800	1.42	4.70	8.51E-19	1.37E-04
1000	1.18	4.60	9.63E-03	1.60E-04
1200	9.93E-01	4.49	2.27E-02	1.79E-04
1400	8.75E-01	4.37	3.02E-02	1.94E-04
1600	7.94E-01	4.24	3.61E-02	2.04E-04
1800	7.36E-01	4.10	4.25E-02	2.10E-04
2000	6.95E-01	3.95	4.70E-02	2.14E-04
2200	6.57E-01	3.80	5.34E-02	2.15E-04
2400	6.31E-01	3.66	5.93E-02	2.15E-04
2600	6.14E-01	3.51	6.21E-02	2.13E-04
2800	6.00E-01	3.36	6.54E-02	2.09E-04
3000	5.98E-01	3.22	6.56E-02	2.06E-04

{Cr_2Er_2}				
H / T	χ_S / cm^3mol^{-1}	χ_T / cm^3mol^{-1}	α	τ / s
400	1.97	6.62	4.00E-02	2.18E-04
600	1.15	6.51	8.54E-02	3.38E-04
800	8.66E-01	6.36	1.03E-01	4.67E-04
1000	7.47E-01	6.15	1.09E-01	5.95E-04
1200	6.66E-01	5.91	1.10E-01	7.04E-04
1400	6.08E-01	5.65	1.09E-01	7.89E-04
1600	5.61E-01	5.37	1.11E-01	8.46E-04
1800	5.32E-01	5.09	1.12E-01	8.84E-04
2000	5.09E-01	4.80	1.13E-01	9.03E-04
2200	4.92E-01	4.53	1.15E-01	9.09E-04
2400	4.78E-01	4.26	1.17E-01	9.05E-04
2600	4.71E-01	4.00	1.16E-01	8.94E-04
2800	4.63E-01	3.76	1.18E-01	8.78E-04
3000	4.55E-01	3.53	1.20E-01	8.56E-04

Table S8. Broken symmetry and high spin states computed at DFT level for complexes **4**-**8**.

4					
	spin density				**energy /hartrees**
	Tb1	**Tb 1'**	**Cr1**	**Cr1'**	
HS	6.016093	6.016050	3.104876	3.104795	-29410.63983473
BS1	6.018269	6.016785	**-3.107343**	3.105501	-29410.64017623
BS2	**-6.018464**	6.015578	3.106202	3.105222	-29410.64017716
BS3	**-6.016293**	6.016314	**-3.106023**	3.105930	-29410.64021615
BS4	6.017778	**-6.017767**	**-3.106917**	3.106839	-29410.64012706
5					
	spin density				**energy /hartrees**
	Ho1	**Ho1'**	**Cr1**	**Cr1'**	
HS	4.000534	4.002762	3.103485	3.104505	-31301.11931970
BS1	3.999855	4.003771	**-3.107191**	3.105306	-31301.11947238
BS2	**-3.998744**	4.002054	3.104722	3.104761	-31301.11944560
BS3	**-3.999416**	4.003081	**-3.105951**	3.105563	-31301.11945153
BS4	3.997781	**-4.001530**	**-3.105547**	3.105799	-31301.11941866

6					
	spin density				**energy /hartrees**
	Er1	**Er1'**	**Cr1**	**Cr1'**	
HS	3.003092	3.009057	3.104745	3.104129	-32281.79495600
BS1	3.000502	3.009736	**-3.104085**	3.104945	-32281.79507967
BS2	**-3.002126**	3.007022	3.105073	3.103894	-32281.79504783
BS3	**-3.004728**	3.007701	**-3.103754**	3.104712	-32281.79510591
BS4	3.001281	**-3.004070**	**-3.105888**	3.104594	-32281.79511339

7					
	spin density				**energy /hartrees**
	Tm1	**Tm1'**	**Cr1**	**Cr1'**	
HS	1.998946	1.992704	3.102873	3.103334	-33286.55742161
BS1	1.994434	1.992736	**-3.103745**	3.104136	-33286.55757689
BS2	**-1.994709**	1.991474	3.102990	3.103580	-33286.55748954

BS3	**-1.999217**	1.991507	**-3.103626**	3.104389	-33286.55753619
BS4	1.994044	**-1.986478**	**-3.103789**	3.103223	-33286.55757947

8					
	spin density				**energy /hartrees**
	Yb1	**Yb1'**	**Cr1**	**Cr1'**	
HS	0.982220	0.982205	3.102138	3.102069	-34315.90584382
BS1	0.974876	0.981710	**-3.103013**	3.102846	-34315.90599609
BS2	**-0.974427**	0.982301	3.102431	3.101851	-34315.90600034
BS3	**-0.981821**	0.981807	**-3.102707**	3.102640	-34315.90596745
BS4	0.974950	**-0.974948**	**-3.103213**	3.103144	-34315.90602360

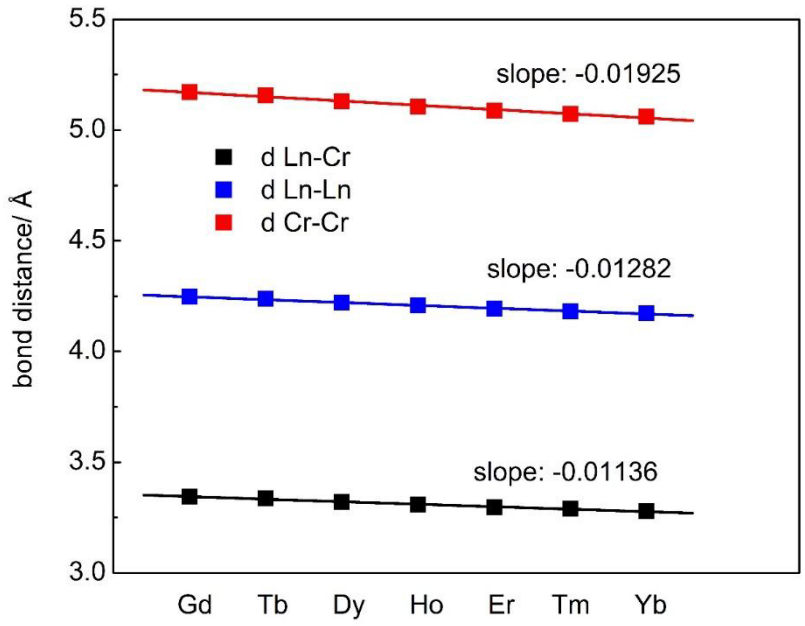

Figure S1. Intramolecular meta-metal bond distance trends along lanthanide series of $Cr^{III}_2Ln^{III}_2$ complexes. For slope calculations, the *x*-axis is simply in increasing units from 1 to 7.

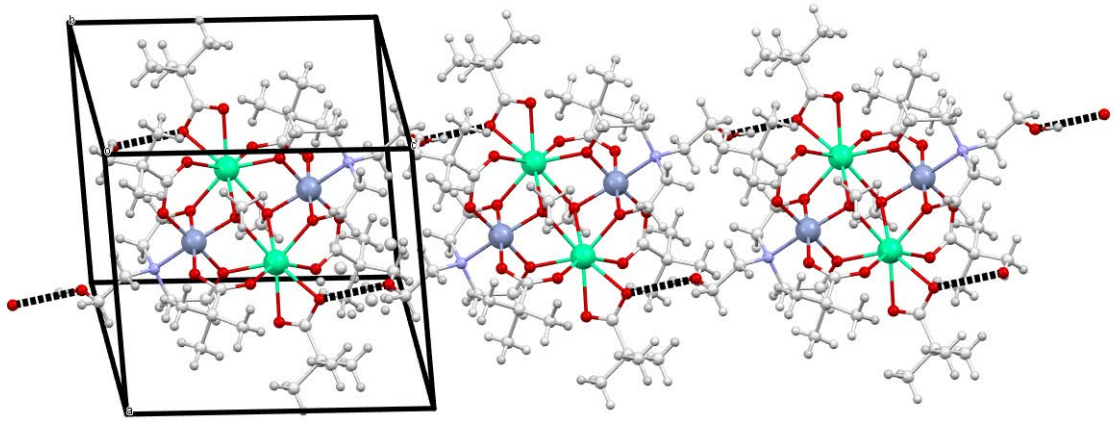

Figure S2. Crystalline packing of complex **4**, the H-bond interactions are shown in black.

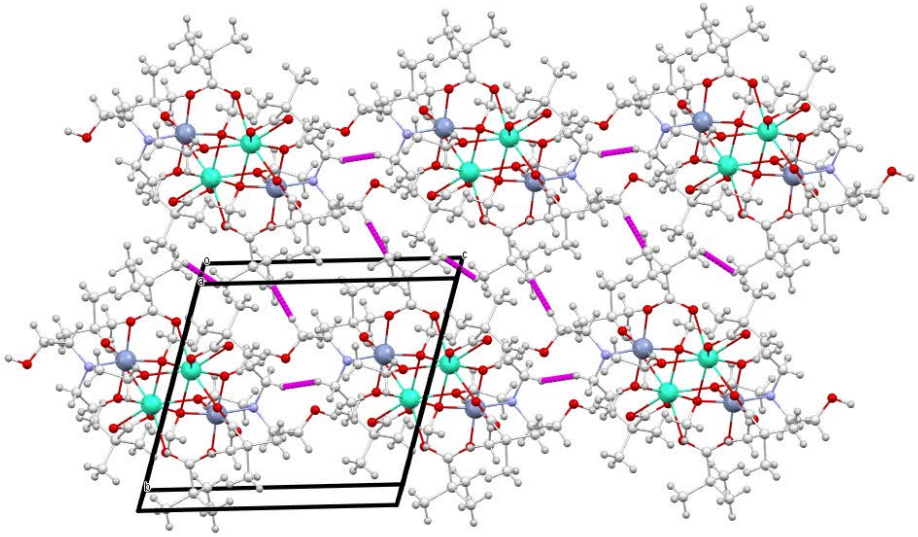

Figure S3. Crystalline packing of complex **4**, the C-H...C-H interactions are shown in magenta.

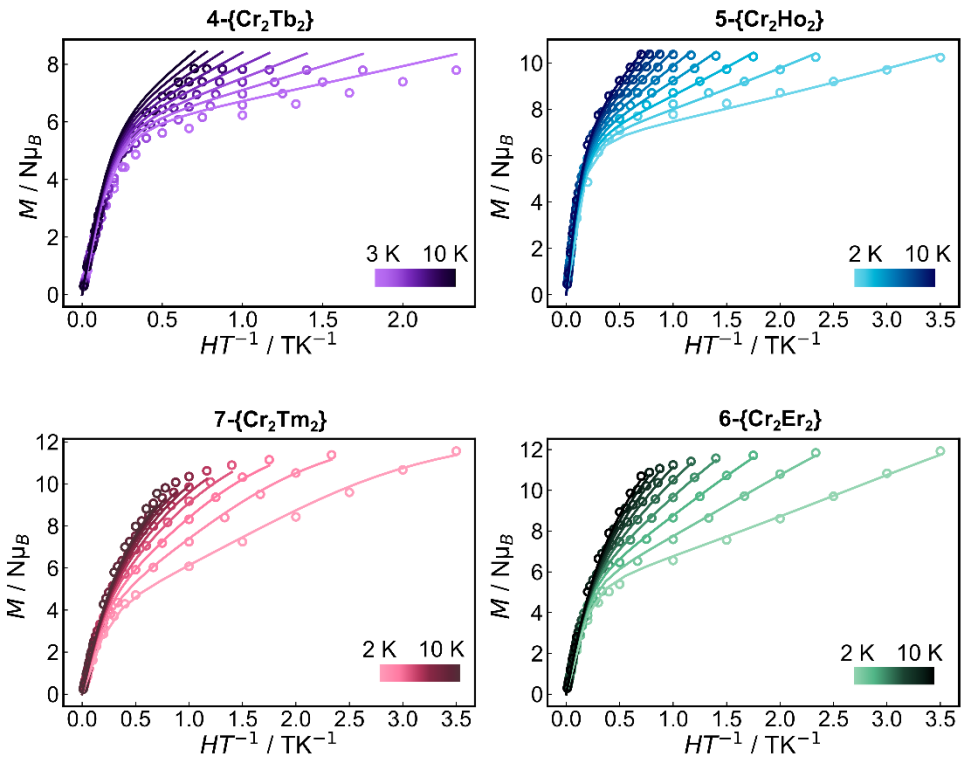

Figure S4. Reduced magnetization data of complexes **4-8.** Open symbol: experimental; full line: simulated according to model described in the text.

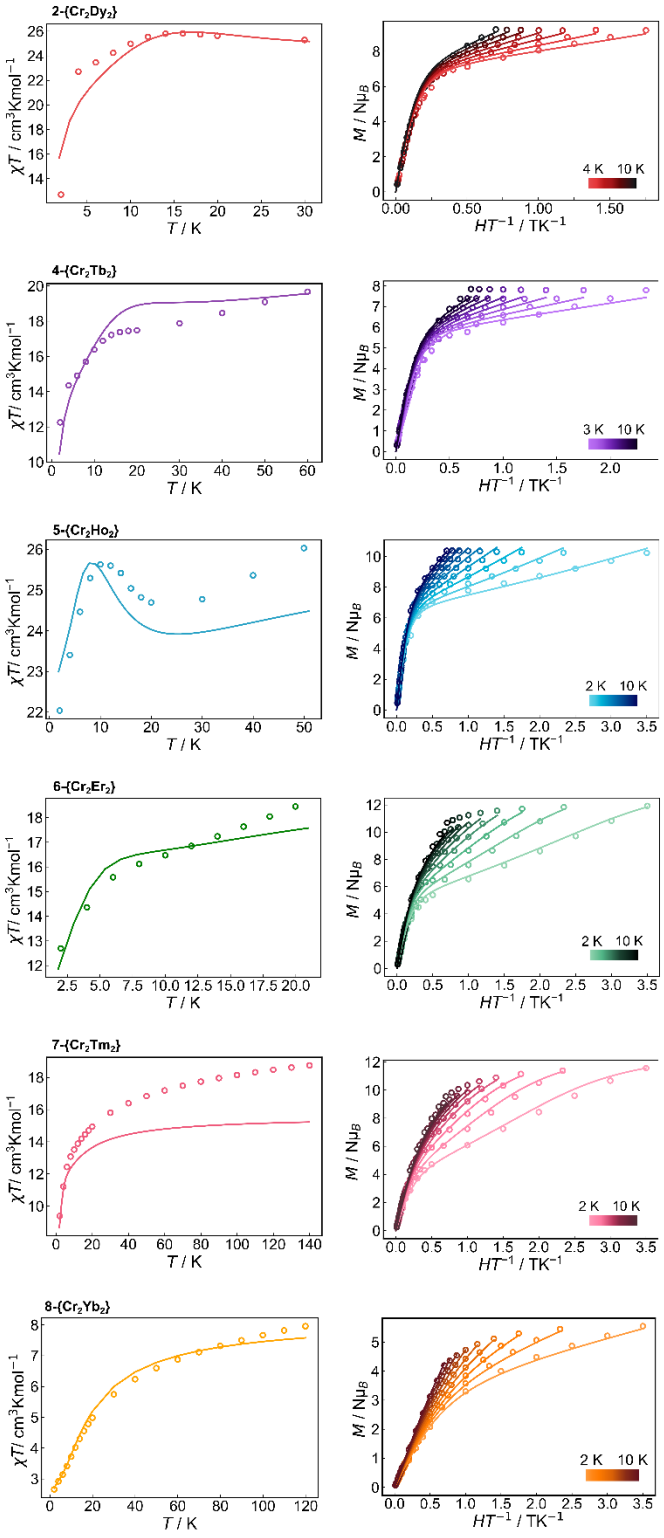

Figure S5. Left: χT vs. T data plot at 0.1 T DC magnetic field of complexes **2** and **4-7**. Right: Reduced magnetization data of complexes **2** and **4-7**. Open symbols: experimental data; full lines: data simulated with the PHI program according to the Hamiltonian specified in the text.

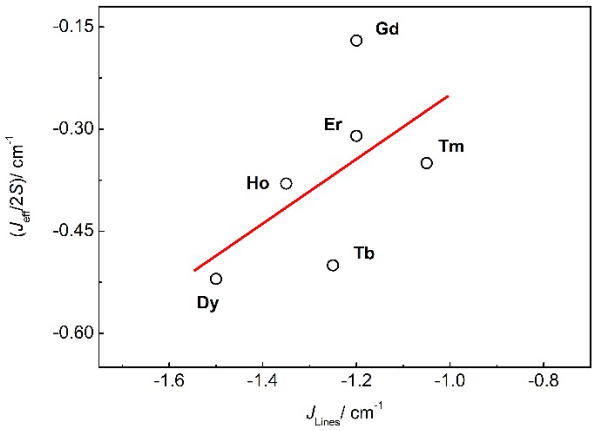

Figure S6. Correlation between experimental $J_{Ln\text{-}Cr}$ isotropic exchange parameter obtained through the Lines approximation and the S_{eff}=1/2 for Ln(III) ion approximation of $Cr^{III}_2Ln^{III}_2$ family (without Yb complex).

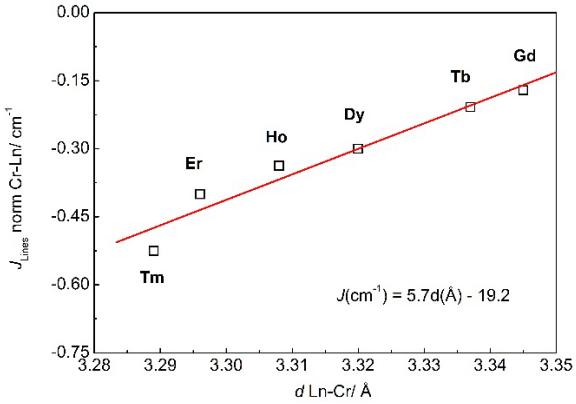

Figure S7. Correlation between experimental $J_{Ln\text{-}Cr}$ isotropic exchange parameter obtained through the Lines approximation and the Ln-Cr bons distance of $Cr^{III}_2Ln^{III}_2$ family (without Yb complex). J_{Lines} norm = J_{Lines}/m with m= number of magnetic orbitals of Ln(III) ions.

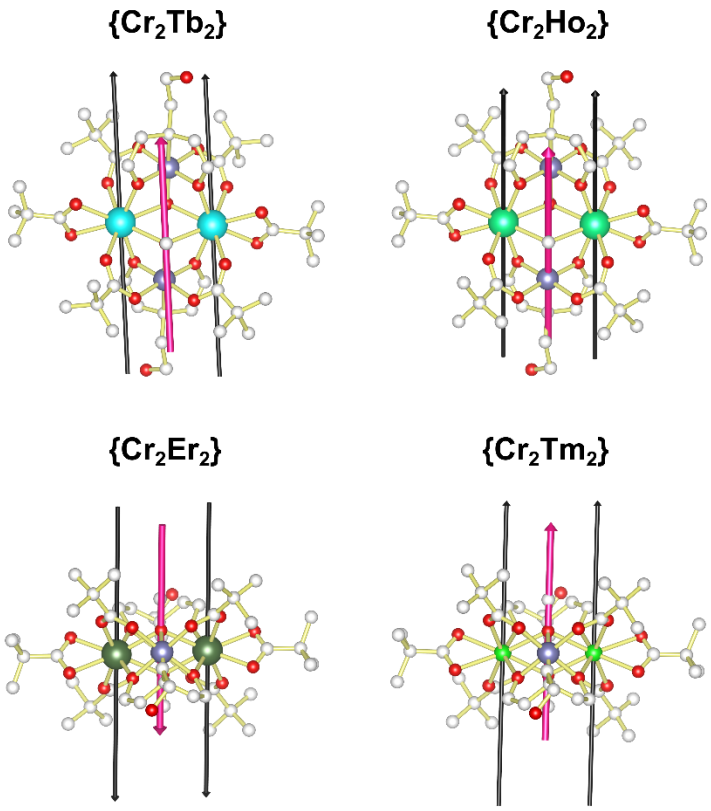

Figure S8. Local Ln(III) main axis orientation (black lines) and ground doublet g-tensor orientation of the exchange system (pink arrow, arbitrarily located over O atom of bridging -OCH_3 ligand) in complex 2.

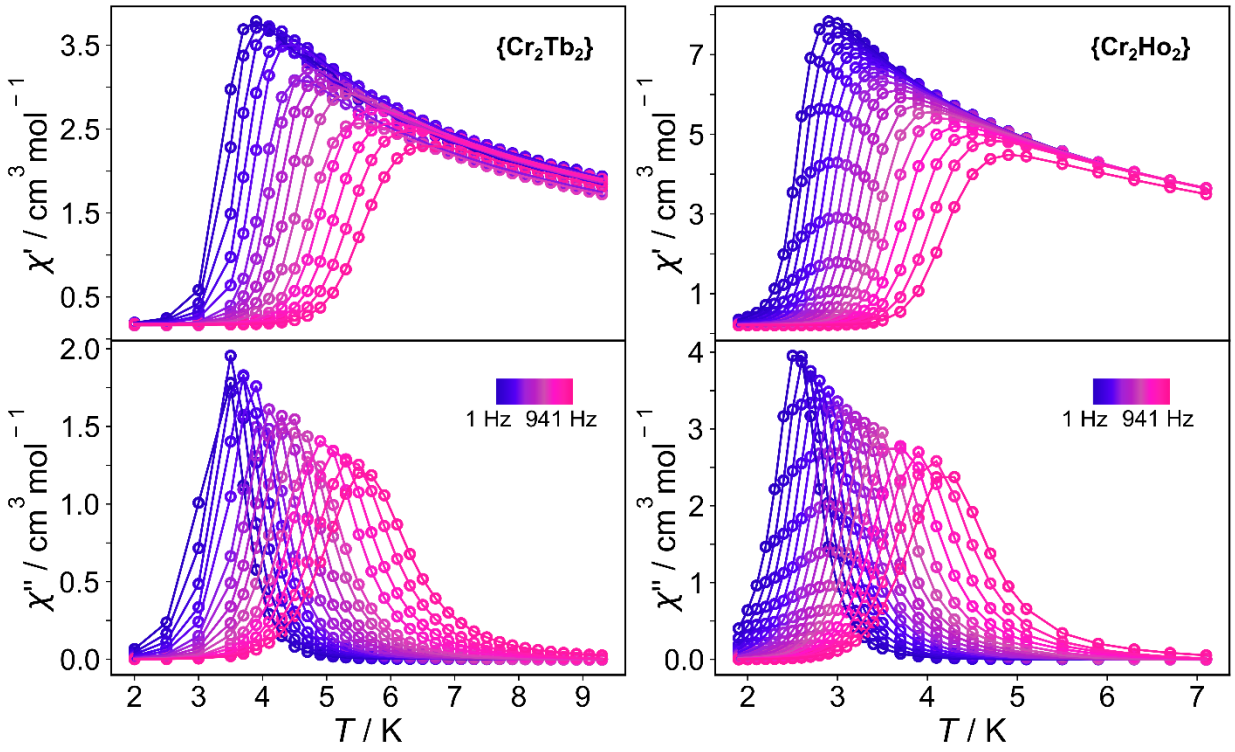

Figure S9. AC magnetic susceptibility data of complexes **4**-**5** at zero applied magnetic field DC at variable temperature and variable frequency (1-941 Hz). Lines are only drawn as eye guideline.

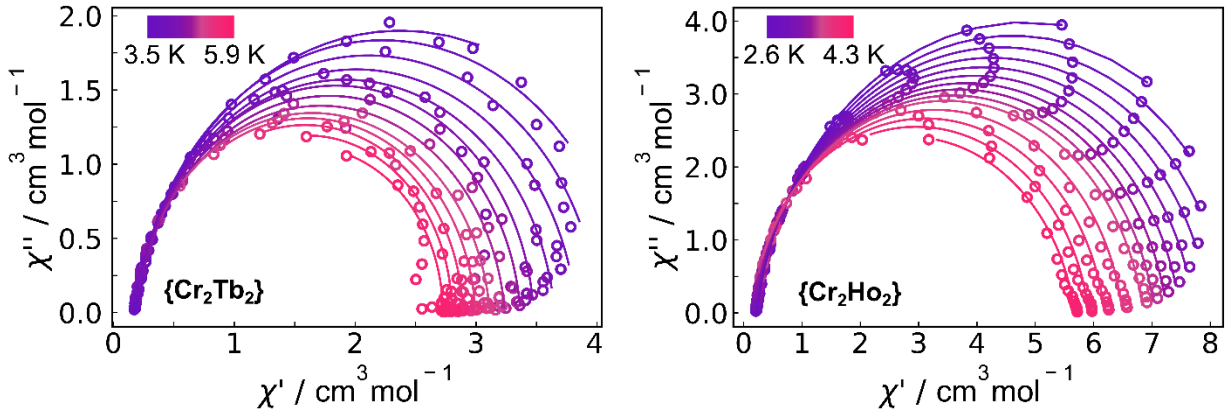

Figure S10. Cole-Cole plots of AC magnetic data for complexes **4**-**5** at 0 Oe. Open symbols: experimental data; full lines: simulated data with generalized Debye model (see text).

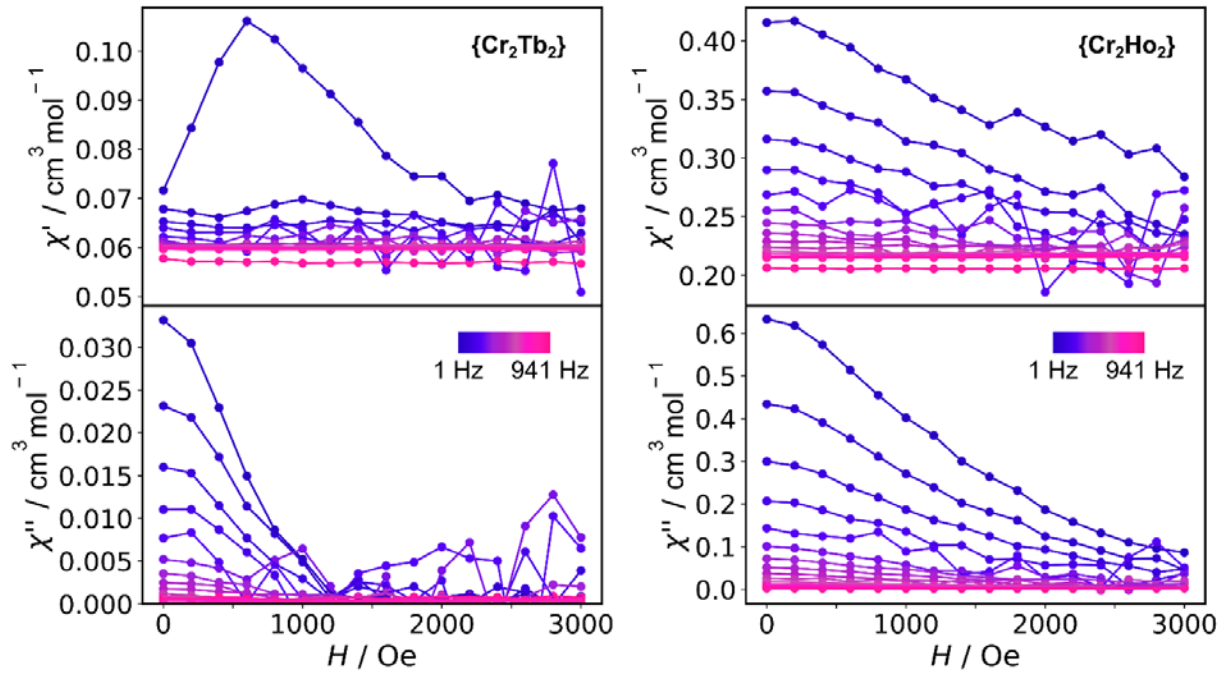

Figure S11. AC magnetic susceptibility data of complexes **4-5** at 2 K under DC applied magnetic field (0-3 kOe) and variable frequency (1-941 Hz). Lines are only drawn as eye guidelines.

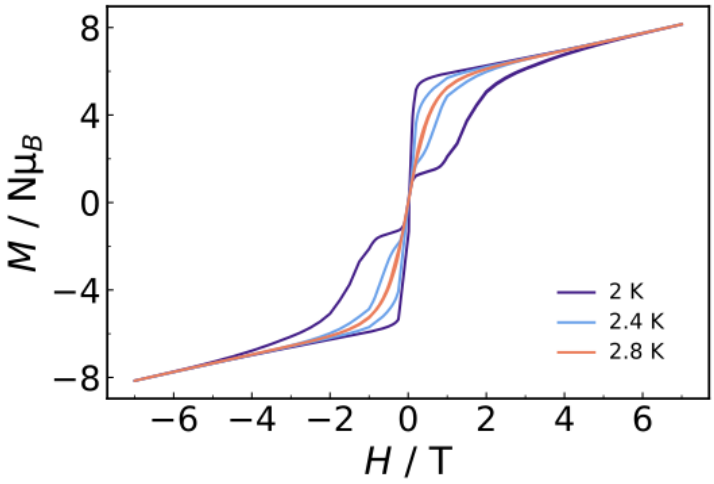

Figure S12. Magnetization hysteresis plots of complex **4**. Field scan rate: 0.007 Ts^{-1}.

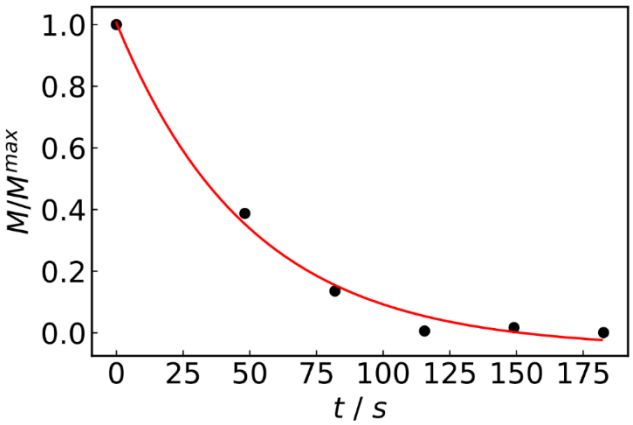

Figure S13. Complex **4** magnetization relaxation at 2 K after applying an external DC field of 1000 Oe and switching it off. Open symbol: experimental; full line: fitting with a mono exponential decay (see text).

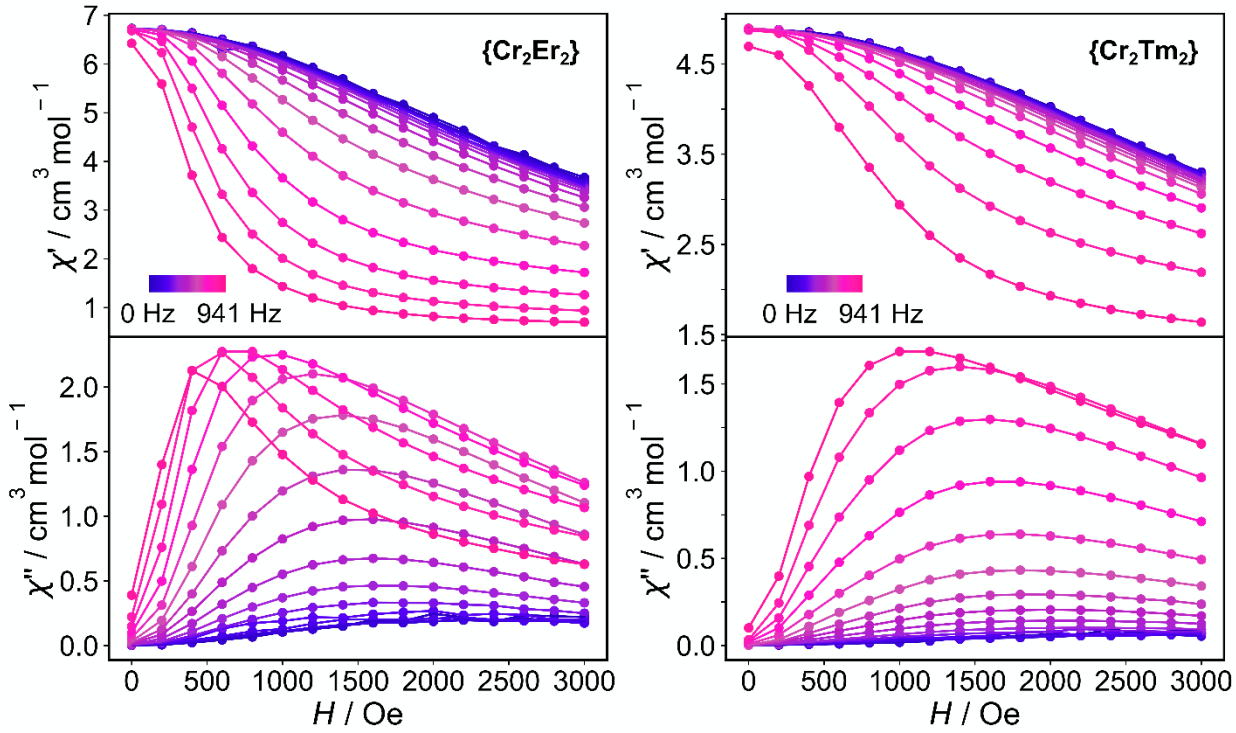

Figure S14. AC magnetic susceptibility data of complexes **6-7** at 2 K under DC applied magnetic field (0-3 kOe) and variable frequency (1-941 Hz). Lines are only drawn as eye guidelines.

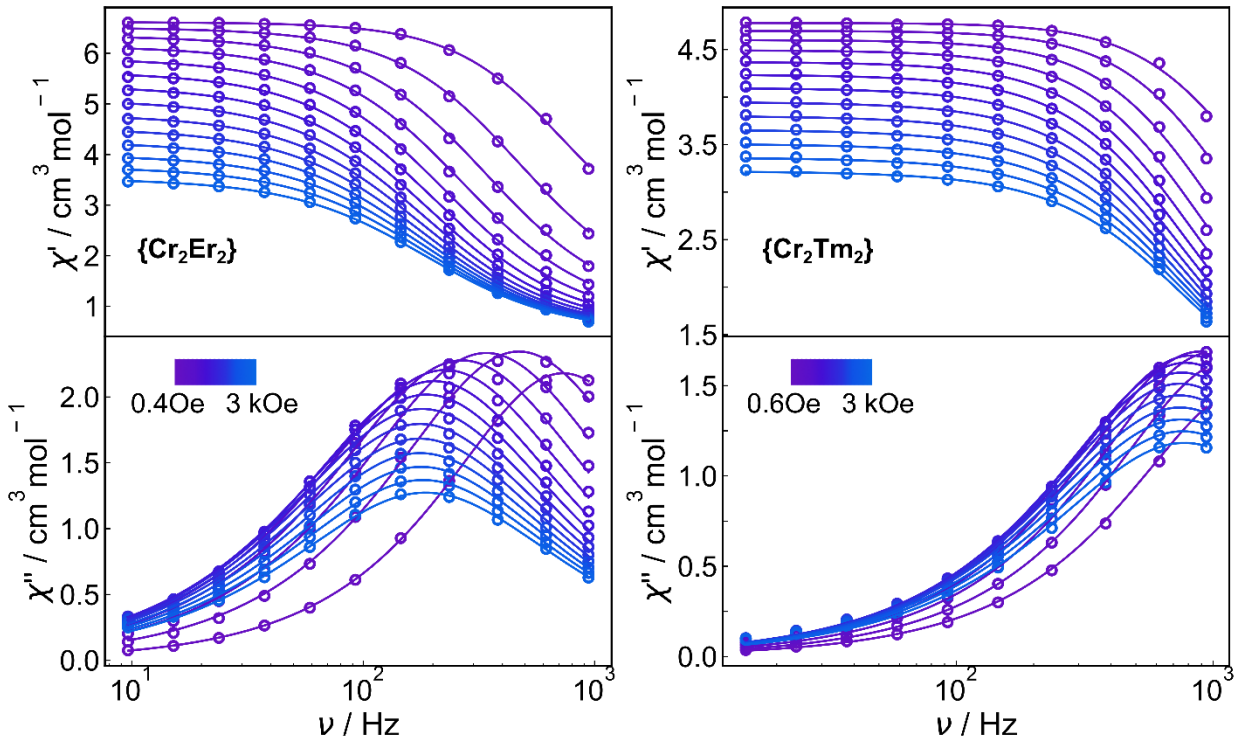

Figure S15. χ'' and χ' frequency dependence at variable field under 2 K of complexes **6-7**. Open symbols: experimental data; Full lines: simulated data with a generalized Debye model (see text).

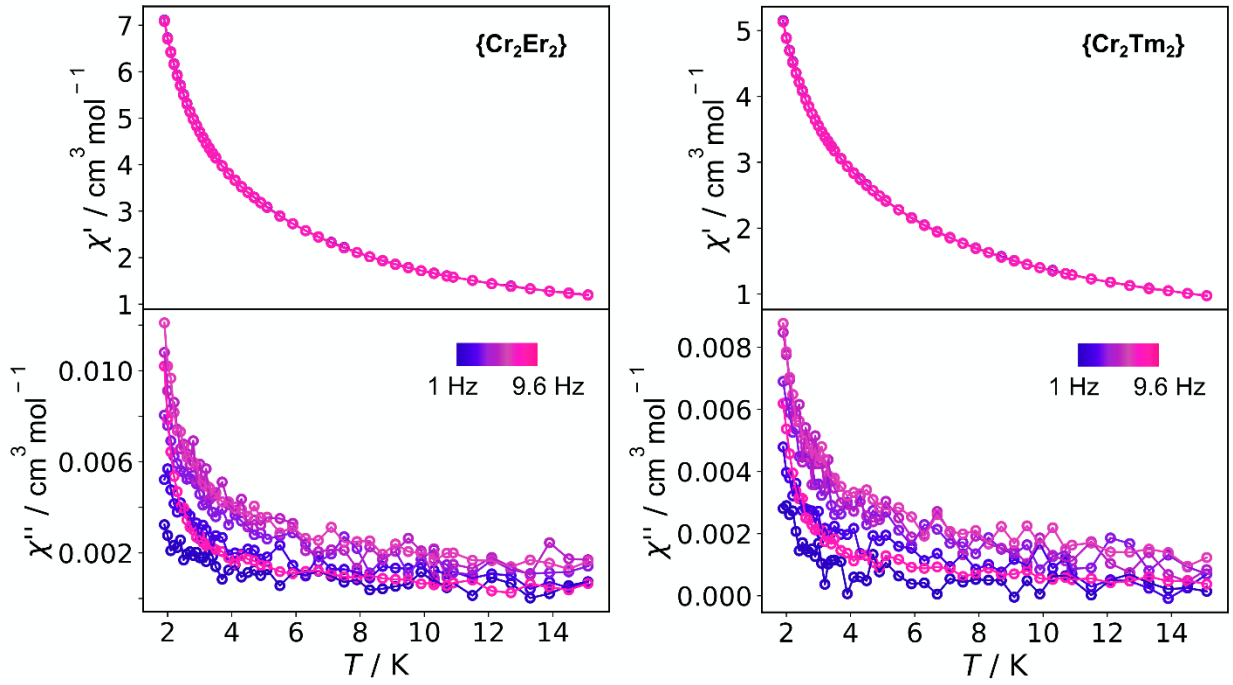

Figure S16. AC magnetic susceptibility data of complexes **6-7** at zero applied magnetic field DC at variable temperature and variable frequency (1-9.6 Hz). Lines are only drawn as eye guidelines.

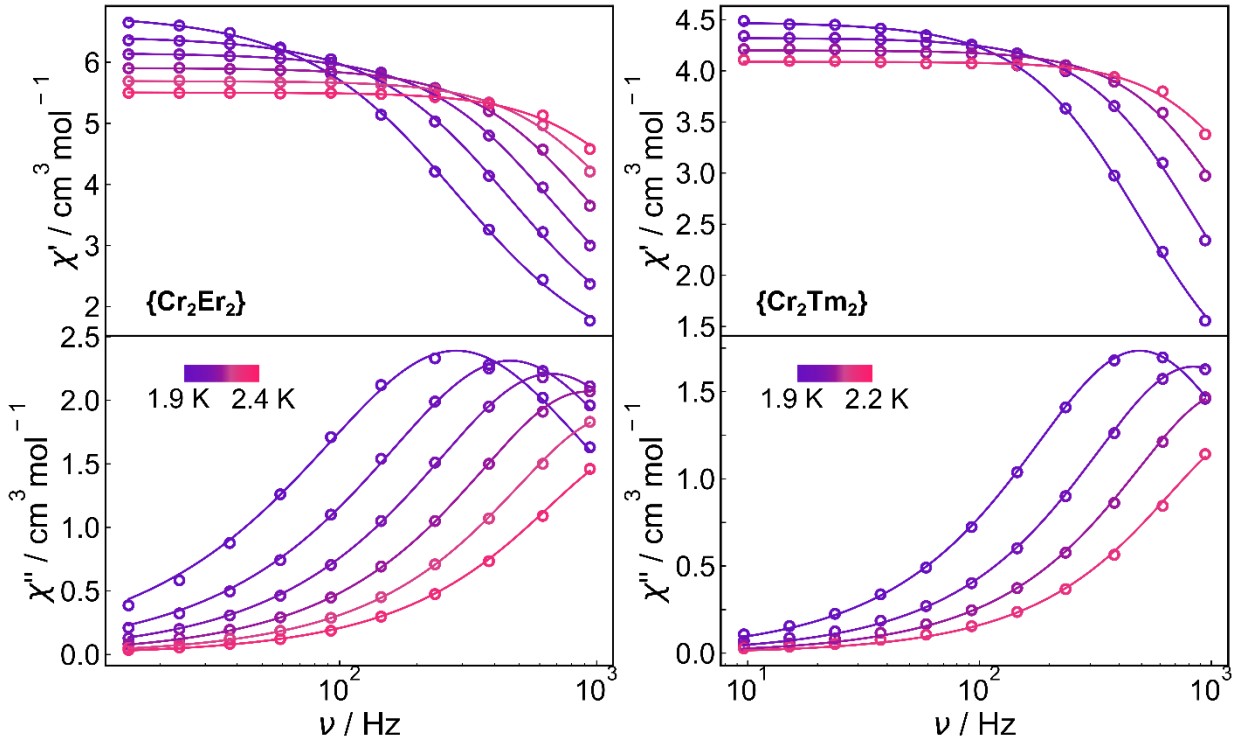

Figure S17. χ'' and χ' frequency dependence at variable temperature under applied field of complexes **6-7**. Open symbols: experimental data; Full lines: simulated data with a generalized Debye model (see text).

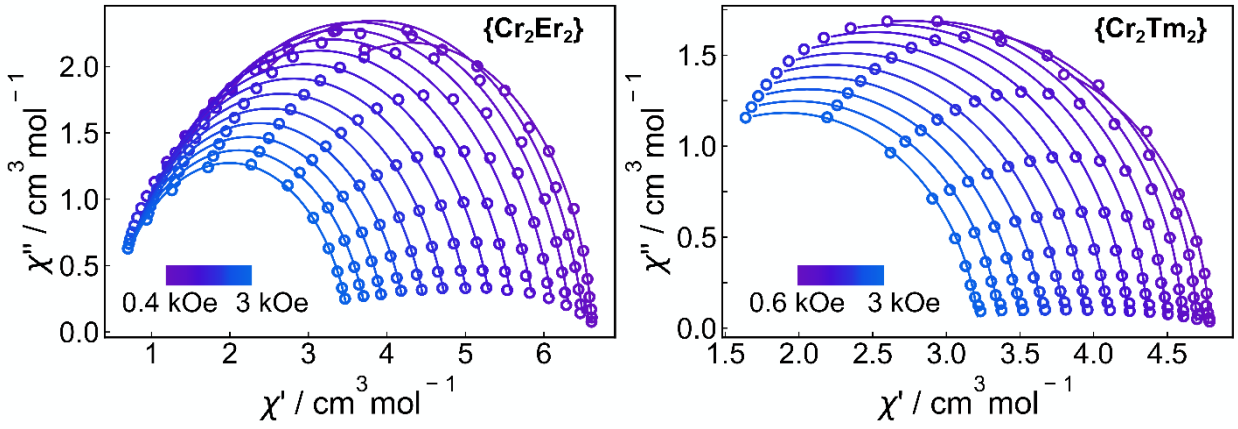

Figure S18. Cole-Cole plots of AC magnetic data for complexes **6-7** at 2 K. Open symbols: experimental data; full lines: simulated data with generalized Debye model (see text).

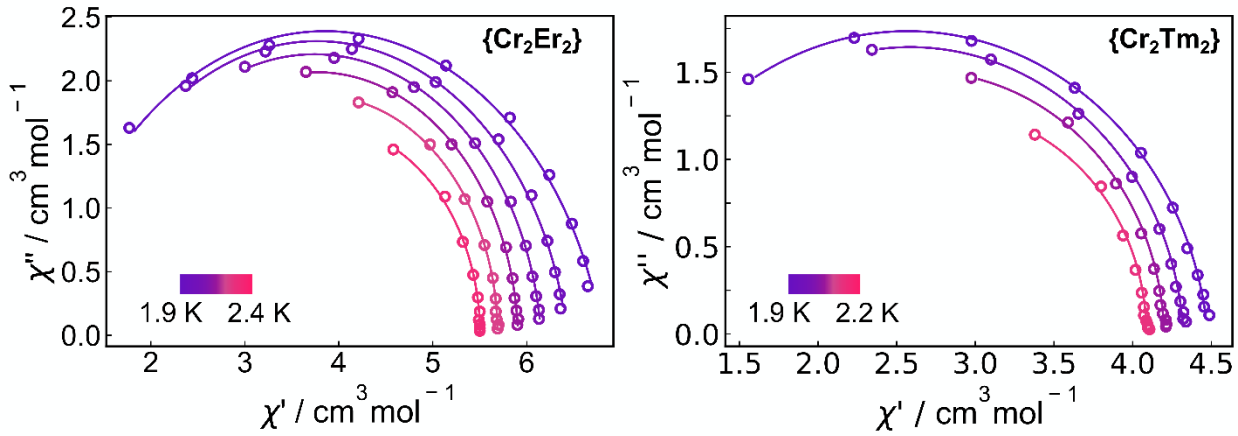

Figure S19. Cole-Cole plots of AC magnetic data for complexes **6** at 1400 Oe and **7** at 600 Oe. Open symbols: experimental data; full lines: simulated data with generalized Debye model (see text).

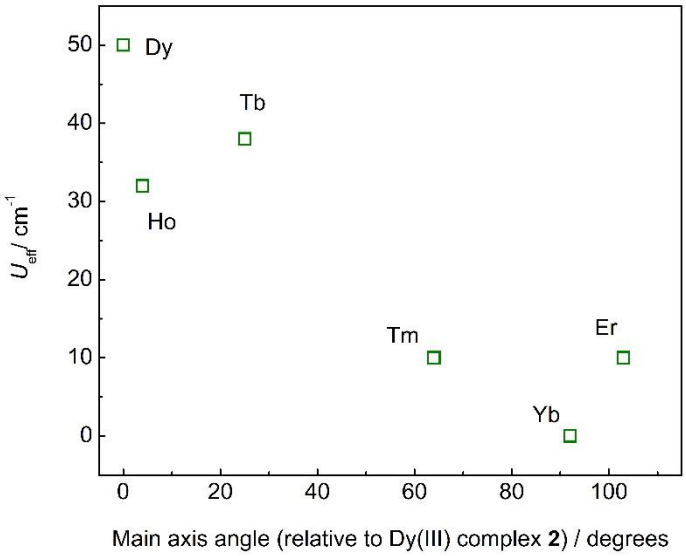

Figure S20. Correlation between U_{eff} and *ab-initio* calculated main magnetization axis orientation relative to Dy(III) complex **2** along the $Cr^{III}_2Ln^{III}_2$ family. $Cr^{III}_2Yb^{III}_2$ complex thermal barrier was set arbitrarily to zero as no SMM behaviour was detected in AC magnetic experiments.